Journal of Electron Spectroscopy and Related Phenomena 173 (2009) 44–49

Contents lists available at ScienceDirect

Journal of Electron Spectroscopy and Related Phenomena

journal homepage: www.elsevier.com/locate/elspec

Optimization of analysis of soft X-ray spectromicroscopy at the Ca 2p edge

S. Hanhan, A.M. Smith, M. Obst, A.P. Hitchcock*

Dept. of Chemistry and BIMR, McMaster University, 1280 Main St W, Hamilton, ON, Canada L8S 4M1

ARTICLE INFO

Article history:
Received 1 February 2009
Received in revised form 15 April 2009
Accepted 20 April 2009
Available online 3 May 2009

Keywords:
NEXAFS
STXM
Absorption saturation
Biofilms
Ca 2p
Calcite
Aragonite

ABSTRACT

Absorption saturation frequently occurs in X-ray absorption spectroscopy whenever transmission detection is used and the sample is too thick. This can strongly distort X-ray absorption spectra, particularly for transitions which have very high intensity and narrow line width relative to the instrumental resolution. This problem is particularly severe at the strong 2p → 3d resonances at the Ca 2p edge, such that there are detectible absorption saturation effects for mineral samples as thin as 30 nm. We describe methods to identify such spectral distortion in scanning transmission X-ray microscopy (STXM) and avoid its effects when generating reference spectra by selecting spatial regions with undistorted spectra. We also show that taking absorption saturation into account is critical when STXM is applied to systems with thick regions. We outline an approach which can provide accurate thickness maps even in the regions where the thickness is such the absorption is saturated at the resonance peaks. Environmental samples such as biofilms, soil samples, sediments, and precipitates are typically heterogeneous in both composition and thickness. They often contain regions thicker than the saturation threshold, yet one would still like to analyse such samples correctly and quantitatively. By excluding the peak energies where absorption saturation distortion occurs, we show it is possible to achieve a meaningful quantitative analysis. We demonstrate the advantages of this approach in the context of mapping two different $CaCO_3$ species biomineralized within a natural river biofilm.

1. Introduction

In every optical technique spectral distortion associated with absorption saturation may occur whenever the path length of light through a sample is too long. In soft X-ray absorption spectroscopy this is primarily an issue when spectra are recorded using transmission detection, but absorption saturation is also known to affect yield-based measurements such as fluorescence yield and even total electron yield [1,2]. Fig. 1 is a cartoon outlining various effects which lead to spectral distortion under conditions of absorption saturation. Light is not always spectrally pure and it always has a finite energy bandwidth. Both aspects depend on details of the optical system. In typical synchrotron experiments, incoming soft X-rays of first and higher orders are incident on the sample. The variable density band inside the sample represents the attenuation of the monochromatic 1st order X-rays caused by the excitation of specific core → valence transitions in the sample. The transmission signal and the observed (solid) and true (dashed) absorbance signals (also called optical density or OD) are shown at the right of the cartoon. At energies where absorption saturation occurs the observed signal at the resonance peak is much smaller than the true signal. This is because the wings of the first order light and the second (or other higher order) light are still detected even though the sample thickness and density are such that all of the first order light is absorbed in the sample. Without spectrally analyzing the detected light, that measured residual transmitted signal (plus any background signals from stray light or electronic issues) is interpreted as transmitted first order light which gives an erroneously low absorbance. This effect is often compounded by detectors being more sensitive to higher energy (second or higher order) light. Effectively there is a large difference in the relative amounts of the spectral components transmitted between on and off the resonance. At some sample thicknesses all of the first order light may be absorbed by the sample. Accordingly, absorption saturation is particularly common when there are sharp, intense transitions, as occurs in Ca 2p spectra [3]. To avoid saturated spectra, it is necessary to keep the sample sufficiently thin and to use as highly monochromated light as possible.

The focus of this work is development of a clear understanding of absorption saturation effects in Ca 2p near edge X-ray absorption fine structure (NEXAFS) spectroscopy [3,4] as measured in a scanning transmission X-ray microscope (STXM) [5–7], and optimization of Ca 2p spectral acquisition to allow determination of the correct spectra of various calcium compounds, both as pure species and in complex heterogeneous environments. Our aim is to develop methods which, even in the presence of severe spectral distortion from absorption saturation, can be used to extract the correct Ca 2p spectral shape for pure, homogeneous materials, and to perform

* Corresponding author. Tel.: +1 905 525 9140; fax: +1 905 521 2773.
E-mail address: aph@mcmaster.ca (A.P. Hitchcock).

0368-2048/$ – see front matter © 2009 Elsevier B.V. All rights reserved.
doi:10.1016/j.elspec.2009.04.010

accurate speciation and quantitative chemical mapping when the calcium 2p edge is used for soft spectromicroscopy in STXM. While only Ca 2p spectra are treated in this study, similar principles will apply to any X-ray absorption edge that has a similar combination of sharp, intense resonance features, and also weak features which have good speciation capability. Other edges where this combination is found include the Ti 2p, Mn 2p, Cr 2p and the 3d edges of rare earth elements. Another example where problems with absorption saturation frequently occur is the C 1s edge. The absorption saturation at this edge is usually associated with strong background absorption by beamline and microscope optics rather than particularly sharp features at the C 1s absorption edge, although these features do occur such as the $1s \rightarrow \pi^*_{C=O}$ transition of carbonates.

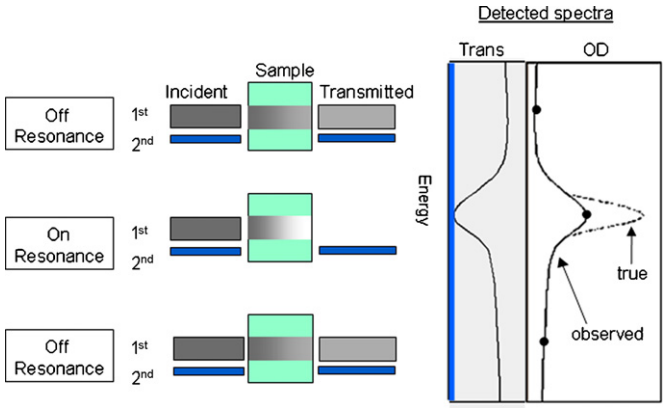

Fig. 1. Cartoon explaining the origin of spectral distortion by absorption saturation. 1st and 2nd refer to the order of the radiation incident upon the sample, which would be 350 and 700 eV for the case of the Ca 2p edge.

2. Experimental

2.1. Samples

The reference samples examined in this work were: calcite in the form of chips of a large single crystal (courtesy of Dr. H.P. Schwarcz), aragonite in the form of crushed, purified abalone shell nacre (courtesy of Dr. J. Rink), $CaCl_2{\cdot}2H_2O$ (Sigma–Aldrich reagent grade, >99.0%) $CaNO_3{\cdot}4H_2O$ (Sigma Ultra, >99.0%), $CaSO_4{\cdot}2H_2O$ (Sigma–Aldrich reagent grade, >99%) and calcium oxalate, $CaC_2O_4{\cdot}H_2O$ (Sigma–Aldrich, >99%). The samples examined by STXM were prepared by grinding in a mortar and pestle and dusting the finely crushed powder onto a Si_3N_4 window (Norcada Inc.). The river biofilm sample was prepared as explained elsewhere [5].

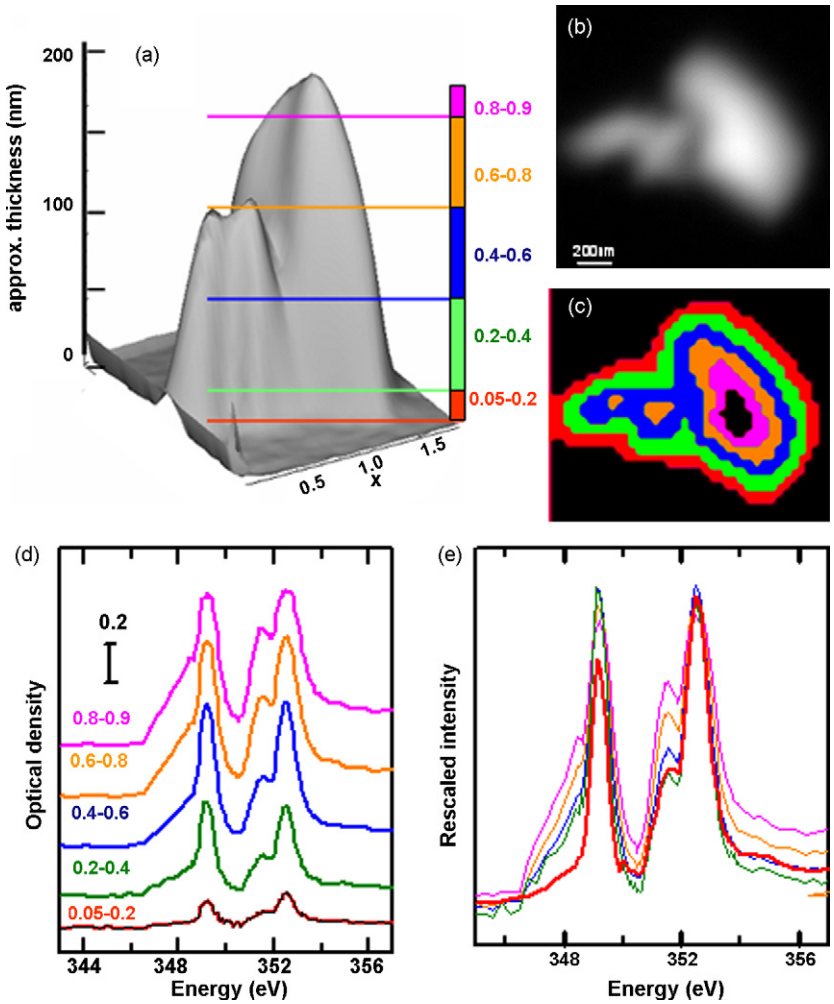

Fig. 2. (a) 3D representation of an image (b) of a crystal of calcium oxalate recorded with STXM, which is the sum of OD images from 344 to 355 eV in a Ca 2p image sequence. (c) Dissecting the calcium oxalate crystal as a function of sample thickness to generate positional masks. (d) Spectra extracted from the corresponding color coded regions (a and c), plotted on an absolute OD scale. Note the significant spectral distortion that occurs for peak ODs above 0.3 OD. (e) Rescaled plot of Ca 2p spectra to show changes associated with absorption saturation (CLS).

2.2. Methods

Soft X-ray spectromicroscopy was carried out using the STXM at beamline 10ID1 at the Canadian Light Source (CLS, Saskatoon, SK) [8] and the polymer STXM at the Advanced Light Source (ALS, Lawrence Berkeley National Laboratory, Berkeley, CA) [9]. Using mirrors, a grating monochromator and a zone plate, soft X-rays are monochromatized and focused onto the sample which is raster scanned while a X-ray detector counts the transmitted X-rays. The STXM instruments used achieve 30 nm spatial resolution which is critical both for measuring spectra of very small regions of appropriate thickness for reference spectroscopy and for investigating Ca carbonate chemistry at fine spatial scale close to the surface of individual bacterial cells or within biofilms. In the absence of absorption saturation distortion, quantitative thickness can be obtained by converting the transmitted intensity to optical density using the Lambert–Beer law. Since STXM is an X-ray in, X-ray out technique and soft X-rays penetrate water except at the O 1s edge, wet samples can be measured [10].

3. Results and discussion

The high spatial resolution of STXM allows one to measure reference spectra from extremely small (sub-micron) regions, and thus to extract undistorted spectra even from samples where the majority of the sample is too thick. Fig. 2 illustrates this for the case of a micron-sized calcium oxalate crystal. A series of images (also called a stack [11]) were recorded at photon energies between 340 and 370 eV. The images were converted to optical density ($OD = \ln(I_0/I)$) using an empty area of the silicon nitride window, adjacent to the sample, as the I_0 region. Fig. 2b is the average of all images, while Fig. 2a presents the same data in a 3d representation. Pixels in ranges of OD values were then selected using aXis2000 software [12]. Setting the threshold to an optical density greater than 0.05 selected the entire sample, whereas optical density greater than 0.2 OD selects the majority of the sample, excluding the thinnest region at the edge of the crystal. Subtracting the two optical density maps (or using a thresholding tool with both minimum and maximum limits [12]), isolates the spectrum from the red ring at the edge of the crystal (Fig. 2c). This procedure was used to identify pixels defining regions of increasing OD over the total OD range of the data. Spectra from each annulus were then extracted and are displayed on an absolute scale in Fig. 2d and in a rescaled representation in Fig. 2e. By comparing the ratios of Ca 2p spectra at different sample thicknesses (OD ranges) it is possible to identify an upper bound to the thickness which avoids absorption saturation. One can then average the spectra from all pixels in regions thinner than that limit in order to obtain a reliable, undistorted reference spectrum. Spectra taken from any of the regions with a peak OD greater than 0.35 were saturated whereas the regions with a peak OD less than 0.25 gave an undistorted spectrum. For this compound and the instrumental conditions used, we conclude that 0.30 ± 0.05 OD is the upper limit for reliable Ca 2p spectra of calcium oxalate. This corresponds to a mineral thickness of about 30 nm. Since the peak OD varies significantly from compound to compound, it is important to make similar evaluations of the absorption saturation limit for each compound studied. We also note that, since absorption saturation arises because the incident light is not spectrally pure and has a finite energy bandwidth (see Fig. 1), the threshold OD for absorption saturation will depend on the beamline used, the spectral response of the detector, and the energy resolution selected.

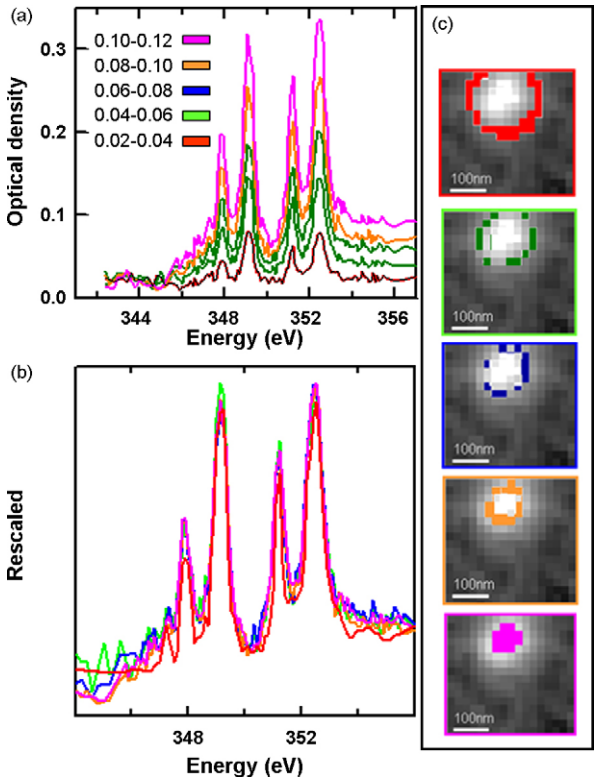

Fig. 3. (a) Spectra plotted on an absolute OD scale, color coded according to region of a very small calcite crystal, (b) calcite spectra rescaled and overlaid for comparison and (c) images of the crystal indicating the regions from which the spectra were extracted (CLS).

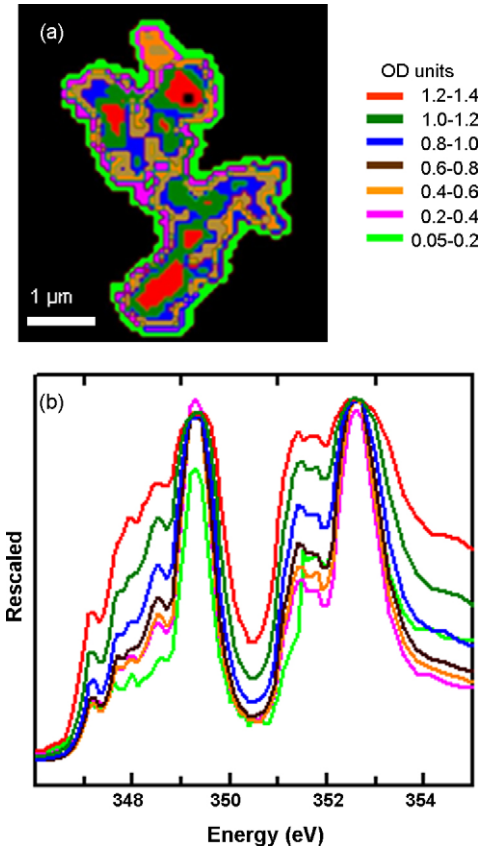

Fig. 4. (a) OD map of a few micron-sized aragonite crystal, with color coded regions of the indicated range of OD for the strongest Ca 2p peak and (b) spectra extracted from the aragonite sample, with rescaled plotting to show the extensive absorption saturation (CLS).

Fig. 3 shows a corresponding analysis for a 175 nm diameter calcite particle. In this case all regions of the particle were sufficiently thin, as is evident from the similarity of the spectra from all thickness ranges—i.e. the intensity of each spectral feature changed linearly with thickness so that the rescaled overplot (Fig. 3b) showed identical spectra, within statistical uncertainties. The spectrum contains a total of seven peaks which are a result of the combination of spin–orbit and crystal-field splitting. The larger splitting into two doublets (L_3 and L_2, with the largest peaks at 349.1(1) and 352.5(1) eV) is the result of the spin–orbit coupling. The peaks are further crystal-field split, by the approximately octahedral field created by the six closest oxygen atoms from the carbonate anions. For each spin–orbit component, this gives rise (in perfect Oh symmetry) to a lower energy triply degenerate state (t_{2g}) and a higher energy, doubly degenerate state (e_g). Together the two main effects create a set of what appears to be four peaks, as two groups of two peaks—{347.9, 349.1 eV} and {351.1, 352.5 eV}. In fact more detailed consideration of the atomic multiplet effects associated with electron–electron repulsion show there are three other very weak peaks, two associated with the L_3 spin–orbit component (346.7, 347.3 eV) and one associated with the L_2 spin–orbit component (351.3 eV), giving rise to the observed seven line spectrum typical of (p^5d^1) configurations in an octahedral environment [13–15].

Fig. 4 shows a corresponding analysis of a much larger (~3 μm wide) aragonite particle. When sufficiently thin regions were examined, it is clear that the spectrum consists of two main components, with a series of much weaker side peaks. However, there was strong spectral distortion by absorption saturation when the peak OD is greater than 0.4, at which point the weaker transitions start to look as strong as the main peaks, since the main peaks are underestimated due to absorption saturation. Thus, what was nominally a 'two-peak' spectrum, became effectively a 'four-peak' spectrum when absorption thickness caused spectral distortion. Since an important differentiation in the field of biomineralization is that between aragonite and calcite [16], it is rather critical that the analysis is not confounded by a change of a 'two-peak' pattern (that of aragonite and many other calcium minerals) into an apparent 'four-peak' pattern (thus similar to the spectrum of calcite) by absorption saturation.

Fig. 5 presents Ca 2p spectra of a set of Ca minerals which were measured to act as reference spectra for biomineralization analysis. In each case care was taken to extract these spectra only from sufficiently thin regions where absorption saturation did not occur. It is clear that, when sufficient care is taken to avoid absorption saturation, there is a large variation among the spectra of different calcium salts. The detailed interpretation of these spectra requires a careful consideration of the ligand field and atomic multiplet effects and is beyond the scope of this paper. However, these spectra clearly show that the fine details of calcium 2p spectra can be very useful for differentiating calcium minerals.

Fig. 6 presents an example of a method we have used to improve the reliability of speciation mapping with the Ca 2p edge, in cases where the sample contains thick regions where absorption satura-

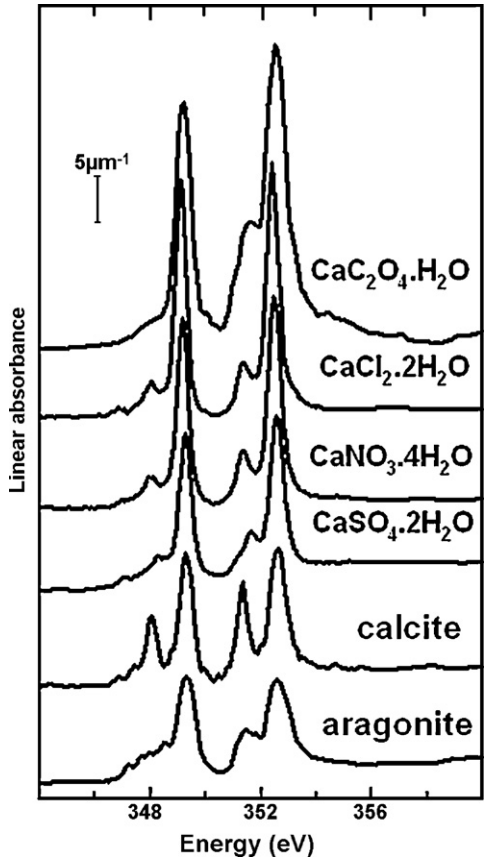

Fig. 5. Spectra of various calcium salts – $CaC_2O_4{\cdot}H_2O$, $CaCl_2{\cdot}2H_2O$, $CaNO_3{\cdot}4H_2O$, $CaSO_4{\cdot}2H_2O$ – and carbonate minerals – calcite and aragonite – acquired from regions tested to be below the absorption saturation threshold. The spectra have been converted to an absolute linear absorbance scale (OD) by adjusting the intensity to match that predicted from the elemental composition and known density, using standard elemental absorption data [20] (CLS and ALS).

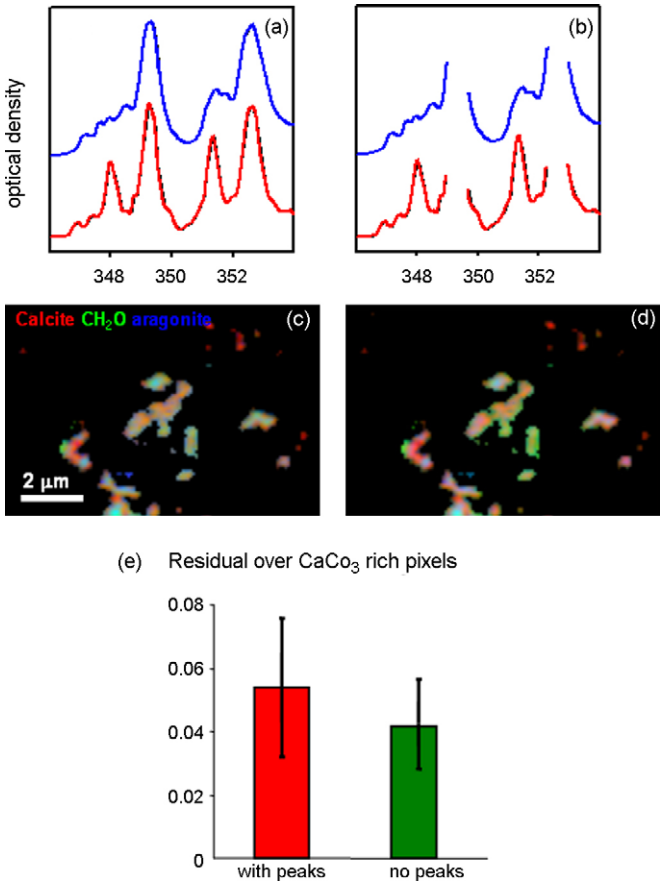

Fig. 6. Illustration of a method to achieve more reliable quantitative speciation mapping by avoiding artefacts from absorption saturation. (a) Calcite (red) and aragonite spectra (blue) including the energy regions of the main Ca L_2 and L_3 resonances and (b) excluding them. (c and d) Resulting species maps of aragonite and calcite for both approaches and (e) residuals of the resulting fits. (For interpretation of the references to color in this figure legend, the reader is referred to the web version of the article.)

tion occurs. Fig. 6a shows the spectra of aragonite (blue) and calcite (red) in the absence of absorption saturation. Normally, the main resonance peaks of the Ca L_3 and L_2 edges would be included in the fit of Ca 2p image sequences. However that could lead to misassignment in cases where the spectra of thicker aragonite-like regions are distorted by absorption saturation and begin to look similar to the "four-peak" spectrum characteristic of calcite (see Fig. 3). In order to avoid this distortion, the images at the energies of the Ca 2p peaks were excluded from the fit, such that the reference spectra used in the fit are those displayed in Fig. 6b. Fig. 6c and d compare the Ca speciation mapping achieved with the full (Fig. 6a) and partial (Fig. 6b) spectral approaches. For simplification all areas except for the precipitates in the biofilm were masked and the minerals were mapped using a singular value decomposition (SVD) algorithm with three components: calcite, aragonite and "CH_2O", a smoothly decreasing signal without any Ca 2p features, which fits the organic carbon in the biofilm. The results of the fits are shown in Fig. 6c and d, respectively. The main difference in the two fits appears in the thickness of aragonite in the central region of the precipitates where the thickness is the highest. The residuals of the two fits are plotted in Fig. 6e. It is clear that the clarity of the mapping (as judged by color purity in the false color composite maps) and the statistical quality of the fit improved when the two main resonance peaks were excluded. Therefore, the remaining minor peaks of the different $CaCO_3$ polymorphs provide sufficient spectral differences to allow for unambiguous chemical mapping. We note that, while removal of the selected energies avoids confusion from the absorption saturated signals, it is also important that there are differences in the remaining spectral features. This is clear when comparing aragonite and calcite, but less so when comparing vaterite and calcite, although a recent study using this method [16] was successful in differentiating these components. We also note that the Ca phosphates are an important geobiological system to which similar arguments apply and the different species successfully discriminated on the basis of their Ca 2p spectroscopy [17].

Fig. 7 shows the final outcome of the Ca 2p-based spectromicroscopy analysis of this region of the biofilm, which was a natural, mixed species biofilm originally from the South Saskatchewan River. Fig. 7b compares spectra extracted from carefully selected regions of this biofilm sample, based on the fitting, in comparison to the reference standards. The specific regions from which undistorted spectra could be obtained are indicated by the color coded discontinuous regions in Fig. 7a, and these regions were identified by thresholding the individual component maps using as guidelines the thickness limits for undistorted spectra deduced from the reference spectral studies (Figs. 3 and 4). Based on this careful analysis and comparison to the accurate reference spectra, we were able to identify and map calcite and aragonite $CaCO_3$ mineral phases, and another species which was identified as Ca^{2+} adsorbed to the extracellular polymers which make up most of the extracellular part of the biofilm. An extensive discussion of mechanisms of formation of $CaCO_3$ mineral phases at the surface of planktonic cyanobacteria is presented elsewhere [16].

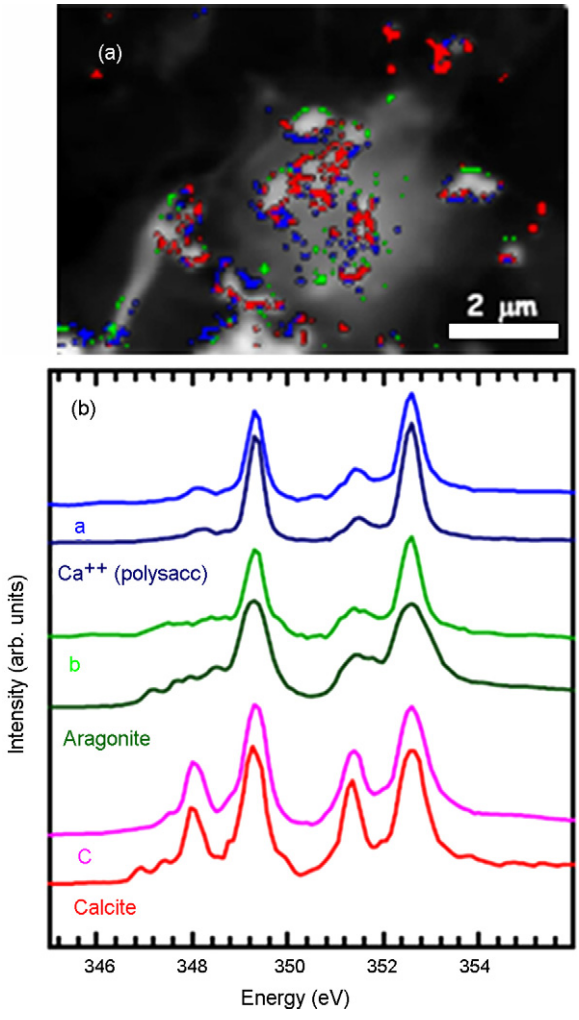

Fig. 7. (a) Sum of images in a Ca 2p sequence recorded from a natural river biofilm. The superimposed color locators—red: calcite-like; green: aragonite-like; blue: Ca^{2+} (polysaccharide-like) are discontinuous regions carefully selected (by threshold masking the individual component maps) to correspond to pixels in regions of relatively pure components which are sufficiently thin to have negligible absorption saturation. (b) Ca 2p spectra extracted from these pixels, compared to spectra of pure calcite, aragonite, and the spectra of all polysaccharide region. (For interpretation of the references to color in this figure legend, the reader is referred to the web version of the article.)

4. Summary

Synchrotron-based scanning transmission X-ray microscopy was used to investigate absorption saturation distortions at intense Ca 2p resonances. Procedures were developed to mitigate the effects of absorption saturation on reference spectra and to improve the accuracy of speciation and chemical mapping. The Ca 2p spectra of several calcium carbonate polymorphs and four calcium salts were derived by these means. These spectra are being used routinely as reference spectra in investigating calcium species adjacent to bacteria undergoing calcium carbonate biomineralization [16,17]. By avoiding the intense peaks which distort at very low sample thickness, it is possible to make meaningful analyses even in thick regions for which the main Ca 2p peaks are badly distorted. A better understanding of Ca 2p spectroscopy recorded in transmission mode will facilitate practical applications of Ca 2p spectromicroscopy with STXM. This is important not only in biomineralization but also other areas, such as studies of cement [18,19] and other biological, environmental and materials systems containing Ca.

Acknowledgements

We thank Jay Dynes for assistance with some measurements. We thank Konstantine Kaznatcheev and Chithra Karunakaran for their excellent work in developing the CLS-SM beamline and STXM, and for providing excellent operational support. Steph Hanhan wishes to thank Lisa Werezak for her support and inspiration. This research was performed primarily at the Canadian Light Source (CLS) which is supported by NSERC, CIHR, NRC and the University of

Saskatchewan. Some spectral data was also collected at STXM 5.3.2 at the Advanced Light Source, which is supported by the Office of Basic Energy Sciences of the US DoE.

References

[1] S. Turchini, R. Delaunay, P. Lagarde, J. Vogel, M. Sacchi, J. Electron. Spectrosc. Relat. Phenom. 71 (1995) 31.
[2] M. Abbate, J.B. Goedkoop, F.M.F. de Groot, M. Grioni, J.C. Fuggle, S. Hofmann, H. Petersen, M. Sacchi, Surf. Interface Anal. 18 (2004) 65.
[3] F.J. Himpsel, U.O. Karlsson, A.B. McLean, L.J. Terminello, Phys. Rev. B 43 (1991) 6899.
[4] J. Stöhr, NEXAFS Spectroscopy, vol. 25, Springer Tracts in Surface Science, 1992.
[5] J.R. Lawrence, G.D.W. Swerhone, G.G. Leppard, T. Araki, X. Zhang, M.M. West, A.P. Hitchcock, Appl. Environ. Microbiol. 69 (2003) 5543.
[6] H. Ade, X-ray spectromicroscopy, in: J. Samson, D. Ederer (Eds.), Experimental Methods in the Physical Sciences, vol. 32, Academic Press, San Diego, 1998.
[7] H. Ade, A.P. Hitchcock, Polymer 49 (2008) 643.
[8] K.V. Kaznatcheev, C. Karunakaran, U.D. Lanke, S.G. Urquhart, M. Obst, A.P. Hitchcock, Nucl. Instrum. Methods A 582 (2007) 96.
[9] A.L.D. Kilcoyne, T. Tylisczak, W.F. Steele, S. Fakra, P. Hitchcock, K. Franck, E. Anderson, B. Harteneck, E.G. Rightor, G.E. Mitchell, A.P. Hitchcock, L. Yang, T. Warwick, H. Ade, J. Synchroton Radiat. 10 (2003) 125.
[10] S. Hanhan, 2006 CLS Annual Report (2007) 117–119.
[11] C. Jacobsen, S. Wirick, G. Flynn, C.J. Zimba, J. Microsc. 197 (2000) 173.
[12] A.P. Hitchcock, aXis2000 is written in Interactive Data Language (IDL), 2008. It is available free for non-commercial use from http://unicorn.mcmaster.ca/aXis2000.html.
[13] F. de Groot, Cood. Chem. Rev. (2004) 1–33.
[14] F. De Groot, A. Kotani, Core Level Spectroscopy of Solids, CRC Press, Boca Raton, FL, USA, 2008.
[15] A.M. Smith, G. Cooper, A.P. Hitchcock, F. De Groot, Phys. Rev. B, in preparation.
[16] M. Obst, J.J. Dynes, J.R. Lawrence, G.D.W. Swerhone, C. Karunakaran, K.V. Kaznatcheev, K. Benzerara, T. Tyliszczak, A.P. Hitchcock, Geochim. Cosmochim. Acta, in press.
[17] K. Benzerara, T.H. Yoon, T. Tyliszczak, B. Constantz, A.M. Spormann, G.E. Brown, Geobiology 2 (2004) 249.
[18] M.C.G. Juenger, P.J.M. Monteiro, E.M. Gartner, G.P. Denbeaux, Cement Concrete Res. 35 (2005) 19.
[19] D.A. Silva, P.J.M. Monteiro, Cement Concrete Res. 36 (2006) 1501.
[20] B.L. Henke, E.M. Gullikson, J.C. Davis, Atomic Data Nucl. Data Tables 54 (1993) 181.